CHINESE OPTICS LETTERS

Vol. 21, No. 3 | March 2023

Inhibition of the aero-optical effects of supersonic mixing layers based on the RVGAs' control

Zihao Xia (夏梓豪)[1**], Haolin Ding (丁浩林)[1,2*], and Shihe Yi (易仕和)[1]

[1] College of Aerospace Science and Technology, National University of Defense Technology, Changsha 410073, China

[2] College of Advanced Interdisciplinary Studies, National University of Defense Technology, Changsha 410073, China

*Corresponding author: dinghaolin_gfkd@foxmail.com

**Corresponding author: summergoings@163.com

Received October 2, 2022 | Accepted November 11, 2022 | Posted Online March 9, 2023

The infrared imaging windows of the hyper/supersonic optical dome are encountering severe aero-optical effects (AOEs), so a flow control device, the ramp vortex generator array (RVGA) is proposed based on the ramp vortex generator to inhibit the supersonic mixing layers' AOE, which is done by the nanotracer-based planar laser scattering technique and ray-tracing method. The experiments prove that under different pressure conditions, RVGA can reduce the mean and standard deviation of the root mean square of the optical path difference (OPD_{rms}) and reduce the supersonic mixing layers' thickness and mixture a great deal. The AOE of the pressure-matched mixing layer is the weakest. Higher RVGA results in better optical performance. RVGA has the potential to be applied to supersonic film cooling to reduce aero-optical aberrations.

Keywords: aero-optical effects; supersonic mixing layer; RVGA; OPD_{rms}; flow control.

DOI: 10.3788/COL202321.030102

1. Introduction

The aero-optical effects (AOEs)[1–3] induced by the supersonic mixing layer structure, which often appear on the surface of a hyper/supersonic optical dome, have attracted a wide range of interest due to their adverse impacts on the imaging quality of infrared imaging windows. The supersonic mixing layers are formed between the surrounding atmosphere and the domes' jet, which are usually used for wall cooling. The AOE is generally summarized as the beam's jitter, blur, bore sight error (BSE), and attenuation of energy. Lawson *et al.*[4] found that the density fluctuation around the optical window of a hypersonic dome is mostly concentrated at the mixing and boundary layers. Spencer and Moore[5] came to similar conclusions: the supersonic mixing layer accounts for nearly 90% of the total AOE around a hypersonic dome. Therefore, finding an effective method to improve the supersonic mixing layer's AOE is an indispensable and urgent need.

Traditional flow control devices include the oscillated flap[6], pulsed injection[7], electromagnetic actuator[8], cavity[9], triangular disturbance[10], lobed mixer[11], and so on. The main problem with those devices is that they mainly aim at enhancing the mixture of the supersonic mixing layer, which is not conducive to the reduction of the AOE.

Recently, some researchers have found that the ramp vortex generator (VG) is a possible way to realize this purpose. Zhu *et al.*[12] studied the AOE of supersonic cooling film over a backward-facing step with VGs at a Mach 3.4 wind tunnel. The optical path difference (OPD) was measured by the wavefront sensor based on the background-oriented schlieren (BOS). They found that the root mean square value of OPD (OPD_{rms}) of the observation field is 0.7317λ in the case without VG control, while with VG control, it is 0.5388λ (λ is the wavelength of incident light). Ding *et al.*[13] investigated the influence of VGs' mitigation on the aero-optical distortion of an optical dome with a Mach 3.0 cooling film at the KD-01 hypersonic gun tunnel (Mach 6.0). The research found that the usage of VGs mitigates the high-order OPD and improves the stability of the distorted wavefront.

Note that the above works focus on typical engineering structures, where the number of VG is only 2 to 3, which may not be enough to improve the whole optical performance of the cooling film. To put forward an in-depth understanding of VGs' improvement on the AOE, we present a new flow control device based on the structure of the VG and name it the ramp vortex generator array (RVGA). The supersonic mixing layer is extracted from the engineering cooling film. The influence of the height of RVGA and pressure conditions of the wind tunnel on the supersonic mixing layer's AOE is thoroughly studied by the nanotracer-based planar laser scattering (NPLS) technique and ray-tracing method. According to the experimental results, RVGA is a promising device that can reduce the thickness and mixture of the supersonic mixing layer, as well as the negative impact of AOE.

2. Experimental Facilities and Methods

The experiments in this paper were conducted in an indraft supersonic mixing layer wind tunnel at the National University of Defense Technology. As shown in Fig. 1, the wind tunnel has a cross-section size of 100 mm × 50 mm and a test section of 250 mm in length, and the total pressure of the upper incoming flows can be adjusted easily by the total pressure adjustor installed at the stabilizing section. Here we define the ratio of static pressure (RSP) as

$$\mathrm{RSP} = P_s^{\mathrm{up}} / P_s^{\mathrm{down}}, \tag{1}$$

where P_s^{up} and P_s^{down} correspond to the static pressure of the upper and the lower flow at the outlet of the nozzle, respectively. Three RSP values were chosen, and the corresponding operating conditions of the wind tunnel are listed in Table 1.

The origin of the coordinates is chosen to be the center of the splitter's trailing edge. The positive direction of the x axis is downstream, the positive direction of the z axis is perpendicular to the splitter, and the y axis is determined by the right-hand rule. The xOz plane is also called the streamwise plane.

The RVGA was mounted at the upper side of the splitter, and its trailing edge was aligned with that of the splitter. A total of three RVGAs with different heights were designed, and each RVGA had 19 tips, 18 notches, and 7 geometrical parameters. h is the height of the RVGA, b is the width of the tip, D is the distance between two adjacent tips, d is the width of the notch, L is the length of the bottom edge, θ is the angle between two adjacent bottom edges, and β is the angle between the upper surface and lower surface. The detailed parameters of the RVGA are shown in Table 2. To avoid bringing too much disturbance to the supersonic mixing layer, the maximum value of h is limited to 2.4δ (δ is the average boundary layer thickness of the splitter's trailing edge). In each operating condition of the tunnel, seven independent experiments were conducted with different RVGA devices and laser sheet positions (parallel to the streamwise plane and overlapping with the tip or notch).

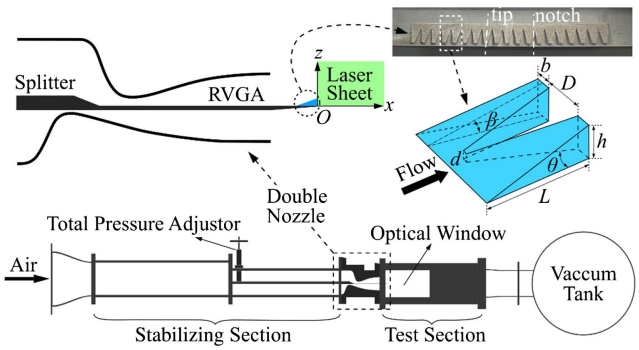

Fig. 1. Supersonic mixing layer wind tunnel and the RVGA device.

Table 1. Wind Tunnel Operating Conditions[a].

	RSP = 1		RSP = 0.72		RSP = 1.21	
	F1	F2	F1	F2	F1	F2
Ma	2.6	3.6	2.6	3.6	2.6	3.6
ρ (kg · m^{-3})	0.035	0.058	0.025	0.058	0.042	0.058
P_0 (kPa)	16.4	101.0	11.8	101.0	19.9	101.0
T_0 (K)	303					
Mc	0.24					

[a]F1 represents the upper flow; F2 represents the lower flow. Ma is Mach number, ρ is density, P_0 is total pressure, T_0 is temperature, and Mc is the convective Mach number.

The detailed flow structures of the mixing layers were captured by the NPLS technique, which is a nonintrusive fine flow field testing technique with a high spatiotemporal resolution and has been widely used in flow visualization of supersonic flow fields[14–17]. Figure 2 shows the NPLS system's layout. The CCD camera with 2048 pixels × 2048 pixels records the images of the flow field, which was illuminated by a thin laser sheet produced by a dual-cavity Nd:YAG laser (wavelength 532 nm, pulse width 6 ns, energy per pulse 350 mJ). The system's optical alignment accuracy can reach 1 mm with the help of moving stages. The noise of the results mainly came from the environmental light and was finally eliminated, since the experiments were carried out during the night.

The density fields of the mixing layer were then acquired by the NPLS-based density measurement technique[18]. Once the density fields are known, we can get the refractive index fields n through the Gladstone–Dale relationship,

$$n = 1 + \rho \cdot K_{\mathrm{GD}}, \tag{2}$$

where K_{GD} is the Gladstone–Dale constant, which is about 2.27×10^{-4} m^3/kg when the light wavelength is 532 nm. Then the aero-optical performance of the mixing layer under different experimental conditions can be studied by the ray-tracing method[2] and evaluated by OPD, which reflects the flow field's influence on the beam quality and is defined as

$$\mathrm{OPD}(t,x) = \int_l n(t,x,z) \cdot \mathrm{d}z - \left\langle \int_l n(t,x,z) \cdot \mathrm{d}z \right\rangle, \tag{3}$$

Table 2. Geometric Parameters of the RVGA[a].

	h (mm)	L (mm)	θ (deg)	β (deg)	D (mm)	b (mm)	d (mm)
RVGA1	0.5	3.20	36.69				
RVGA2	0.8	4.97	23.07	9.33	1.60	0.80	0.10
RVGA3	1.2	7.37	15.50				

[a]Some variables are coupled [$h = L\cos(\theta/2)\tan\beta$] and as many parameters as possible are kept the same.

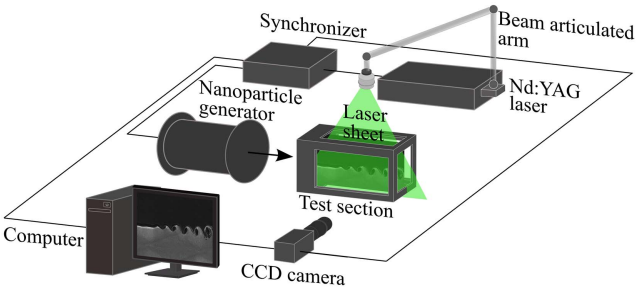

Fig. 2. Schematic diagram of the NPLS system.

where l represents the propagation distance of light in the flow field.

To explain the difference in OPD between various experiments, the Sutton linking equation[19] is applied as

$$\mathrm{OPD}_{\mathrm{rms}}^2 = \alpha K_{\mathrm{GD}}^2 \int_0^l \rho_{\mathrm{rms}}'^2(z)\Lambda(z)\mathrm{d}z. \tag{4}$$

In Eq. (4), rms means the root mean square value, α is a constant, ρ_{rms}' is the density fluctuation, and $\Lambda(z)$ is the correlation length of the density fluctuation. ρ_{rms}' and $\Lambda(z)$ are two important parameters reflecting the flow field's homogeneity, which are defined as

$$\rho_{\mathrm{rms}}' = (\rho - \overline{\rho})_{\mathrm{rms}}, \tag{5}$$

$$\Lambda(z_1) = \frac{1}{2}\int_0^L \frac{\mathrm{cov}_{\rho'}(z_1, z_2)}{\rho_{\mathrm{rms}}(z_1)\rho_{\mathrm{rms}}(z_2)}\mathrm{d}z_2, \tag{6}$$

where ρ is the transient density, $\overline{\rho}$ is the average density, and z_1 and z_2 represent different positions along the direction of light transmission.

3. Results and Discussions

The typical NPLS results (resolution 105 μm/pixel) of supersonic mixing layers with/without RVGA control at different RSP conditions are shown in Fig. 3; the shooting range is $x = 20$–220 mm. The lower part of the mixing layer looks brighter because of its higher density. It is seen clearly that the NPLS results (without RVGA control) under different RSPs have quite distinct forms. When RSP = 1, the mixing layer is flat at the beginning of the mixture, then quickly rolls up to form several Kelvin–Helmholtz (K–H) vortices, and finally breaks up into turbulent flow composed of numerous small vortices. When RSP = 0.72, the mixing layer tilts upward, and the initial mixture process is smoother and longer, after which huge K–H vortices appear and slowly break up. When RSP increases to 1.21, the mixing layer tilts downward and the mixture takes place at the beginning of the image, which implies a stronger mixing process. However, when the RVGAs' disturbance is introduced, the flow field becomes flatter and stabler regardless of the RSP, and the large vortices in the flow field nearly totally vanish. At the same time, the thickness and mixture of the supersonic mixing layers are reduced.

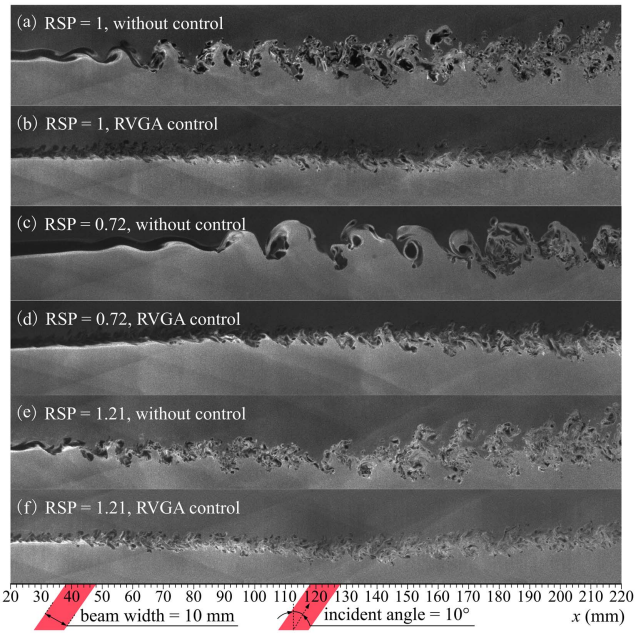

Fig. 3. NPLS images of supersonic mixing layers.

To evaluate the AOE of different cases, we chose a beam with a wavelength of 532 nm and let it traverse through the flow field from $x = 30$ mm to 190 mm in increments of 10 mm. The beam's width and incident angle are illustrated in Fig. 3 and were chosen to reflect a real flight condition[2]. Figure 4 shows the mean and standard deviation (σ) value of $\mathrm{OPD}_{\mathrm{rms}}$ along the streamwise direction, of which the former reflects the average AOE and the latter reflects the AOE's variance with time. The "notch/tip" in the legend represents the laser's illumination position. It should be noted that with RVGA control, the $\mathrm{OPD}_{\mathrm{rms}}$ and $\sigma_{\mathrm{OPD}_{\mathrm{rms}}}$ in all situations have decreased to various extents as well as their distribution curves' fluctuation with the x axis,

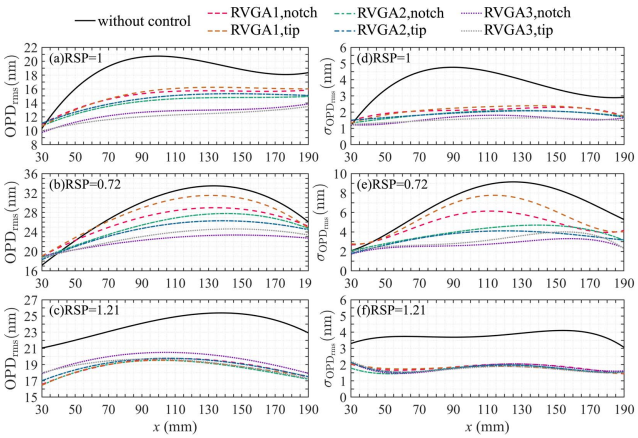

Fig. 4. Mean and standard deviation values of $\mathrm{OPD}_{\mathrm{rms}}$ along the streamwise direction.

which means the beam's AOE is weakened and the beam's quality and stability are improved.

With or without RVGA control, it is found that the OPD_{rms} and $\sigma_{OPD_{rms}}$ are the smallest at RSP = 1 and the largest at RSP = 0.72 in most situations, which means the pressure-matched supersonic mixing layer has the weakest AOE. Then we consider RVGA's influence on the AOE. First, it can be observed that the higher the RVGA is, the more the OPD_{rms} and $\sigma_{OPD_{rms}}$ are reduced, especially seen in Figs. 4(a), 4(b), and 4(e). Second, the AOE at the notch seems to be worse than that at the tip in some cases, but generally, they do not have conspicuous differences. Third, the effect of RVGA's control on the AOE is the best at RSP = 1.21 because an overall decline of the OPD_{rms} and $\sigma_{OPD_{rms}}$ is realized regardless of the RVGA height or the laser sheet position, as well as an excellent and stable control ability.

In order to explain these phenomena, the NPLS images are divided into 10 uniform parts along the streamwise direction to calculate the corresponding ρ'_{rms} and Λ_{max}, which is the maximum of $\Lambda(z)$. Figure 5 shows Λ_{max} and ρ'_{rms} results. The RVGAs' control remarkably reduces the Λ_{max} and ρ'_{rms} in all cases, which implies that the density fluctuations in the flow fields decrease a lot, and the large-scale vortices (such as K–H vortices, which are anisotropic and the main source of the AOE) are diminished effectively. Similarly, it is found that the effect of RVGA's control on the Λ_{max} and ρ'_{rms} is the best at RSP = 1.21, then at RSP = 1, which is a mutual confirmation of the OPD_{rms} results. As shown in Eq. (4), the OPD_{rms} is proportional to Λ and ρ'_{rms}, and that is why the AOE is inhibited by RVGA.

The work above proves that RVGA is a useful tool in controlling the OPD_{rms} of the supersonic mixing layer and has an overall improvement for the aero-optical performance. Higher RVGA gives better control results in our research. The influence of L, θ, β, D, b, and d on the AOE has not been discussed and should be subsequent research priorities. This device's optimization and its availability on a real optical dome will be the aim of future research.

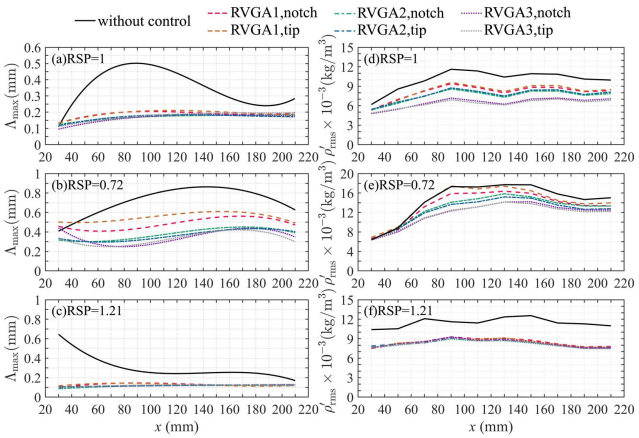

Fig. 5. Distribution of density fluctuation and its correlation length along the streamwise direction.

4. Conclusions

In conclusion, we have developed a flow control device (RVGA) based on the ramp VG. Three RVGAs are successfully applied to mitigate the AOE induced by supersonic mixing layers ($Mc = 0.24$) with different RSPs. The supersonic mixing layers' thickness and mixture are reduced with RVGA control, and the flow fields become more uniform. The AOE of RSP = 1 mixing layer is the weakest and that of RSP = 0.72 mixing layer is the strongest. In addition, the higher the RVGA is, the better the aero-optical performance is. Therefore, this device has great potential in the applications of inhibiting the AOE and mixture of supersonic film cooling.

Acknowledgement

This work was supported by the National Natural Science Foundation of China (No. 12102463), the National Defense Basic Scientific Research Program of China (No. 2022-JCJQ-JJ-1123), and the Natural Science Foundation of Hunan Province (No. 2021JJ40652).

References

1. H. L. Ding, S. H. Yi, Y. Xu, and X. H. Zhao, "Recent developments in the aero-optical effects of high-speed optical apertures: From transonic to high-supersonic flows," Prog. Aerosp. Sci. **127**, 100763 (2021).
2. G. M. Guo, H. Liu, and B. Zhang, "Aero-optical effects of an optical seeker with a supersonic jet for hypersonic vehicles in near space," Appl. Opt. **55**, 4741 (2016).
3. E. J. Jumper and E. J. Fitzgerald, "Recent advances in aero-optics," Prog. Aerosp. Sci. **37**, 299 (2001).
4. S. M. Lawson, R. L. Clark, M. R. Banish, and R. F. Crouse, "Wave-optic model to determine image quality through supersonic boundary and mixing layers," Proc. SPIE **1488**, 268 (1991).
5. A. Spencer and W. Moore, "Design trade-offs for homing missiles," in *Annual Interceptor Technology Conference* (1992), paper AIAA 1992-2755.
6. L. Chew and W. Christiansen, "Coherent structure effects on the optical performance of plane shear layers," AIAA J. **29**, 76 (1991).
7. A. D. Cutler, G. C. Harding, and G. S. Diskin, "High frequency supersonic pulsed injection," in *Annual Interceptor Technology Conference* (2001), paper AIAA 2001-517.
8. D. K. McLaughlin, S. Martens, and K. W. Kinzie, "An experimental investigation of large scale instabilities in a low Reynolds number two-stream supersonic shear layer," in *Annual Interceptor Technology Conference* (1992), paper AIAA 1992-177.
9. A. Zang, T. Tempel, K. Yu, and S. G. Buckley, "Experimental characterization of cavity-augmented supersonic mixing," in *Annual Interceptor Technology Conference* (2005), paper AIAA 2005-1423.
10. S. Watanabe and M. G. Mungal, "Velocity field measurements of mixing-enhanced compressible shear layers: effects of disturbance configuration," in *Annual Interceptor Technology Conference* (2000), paper AIAA 2000-92.
11. D. D. Zhang, J. G. Tan, and J. W. Hou, "Structural and mixing characteristics influenced by streamwise vortices in supersonic flow," Appl. Phys. Lett. **110**, 124101 (2017).
12. Y. Z. Zhu, S. H. Yi, H. L. Ding, W. S. Nie, and Z. W. Zhang, "Structures and aero-optical effects of supersonic flow over a backward facing step with vortex generators," Eur. J. Mech. B Fluids **74**, 302 (2019).
13. H. L. Ding, S. H. Yi, X. H. Zhao, H. X. Xiong, and T. C. Ouyang, "Experimental investigation on aero-optical mitigation of hypersonic optical dome using microvortex generators," AIAA J. **57**, 2653 (2019).

14. Y. X. Zhao, S. H. Yi, L. F. Tian, and Z. Y. Cheng, "Supersonic flow imaging via nanoparticles," Sci. China Technol. Sci. **52**, 3640 (2009).
15. H. L. Ding, S. H. Yi, T. C. Ouyang, and Y. X. Zhao, "Research on velocity measurements of the hypersonic turbulent boundary layer based on the nano-tracer-based planar laser scattering technique," Meas. Sci. Technol. **31**, 085302 (2020).
16. X. Liu, S. Yi, X. Xu, Y. Shi, T. Ouyang, and H. Xiong, "Experimental study of second-mode wave on a flared cone at Mach 6," Phys. Fluids **31**, 074108 (2019).
17. D. Gang, S. Yi, and Q. Mi, "MHz rate flow visualization of the evolution of supersonic compressible mixing layer," J. Vis. **25**, 1117 (2022).
18. L. F. Tian, S. H. Yi, Y. X. Zhao, L. He, and Z. Y. Cheng, "Study of density field measurement based on NPLS technique in supersonic flow," Sci. China Phys. Mech. Astron. **52**, 1357 (2009).
19. H. L. Ding, S. H. Yi, X. H. Zhao, J. R. Yi, and L. He, "Research on aero-optical prediction of supersonic turbulent boundary layer based on aero-optical linking equation," Opt. Express **26**, 31317 (2018).